Pilot–Symbol Based Orthogonal Frequency Division Multiplex Frequency Acquisition Techniques For Dispersive Mobile Channels *

T. Keller*, L. Piazzo†, P. Mandarini†, L. Hanzo*

*Dept. of Electronics and Computer Science,
University of Southampton, SO17 1BJ, UK.
Email:lh@ecs.soton.ac.uk
http://www-mobile.ecs.soton.ac.uk

†INFOCOM Dept.,
University of Rome "La Sapienza"
Email:paolo@acts.ing.uniroma1.it

Abstract

A pilot-tone based reference symbol is proposed for frequency acquisition in time-frame based OFDM systems, and the frequency synchronisation performance is studied in both AWGN and in Rayleigh fading time dispersive channels. The system's BER performance was found to be very close to that of the perfectly synchronised modem.

1 Introduction

In this contribution, we focus our attention on the frequency synchronisation aspects of Orthogonal Frequency Division Multiplex (OFDM) schemes, which were recently adopted for a range of applications, including Digital Audio Broadcasting (DAB), Digital Video Broadcasting (DVB) and for high-rate Wireless Local Area Networks (WLANS). Carrier frequency mismatch between the transmitter and the receiver of an OFDM system introduce inter–subcarrier interference degrading the overall BER performance [1]. We propose a novel frequency synchronisation algorithm that is based on our frame–start reference symbol introduced in Section 2. This reference symbol concentrates the energy in a small set of pilot carriers and therefore supports robust operation at low SNRs over time-dispersive channels, exhibiting negligible BER degradation in comparison to the perfectly synchronised system.

Figure 1 schematically shows the structure of a transmission frame for WLAN TDD/TDMA system, consisting of a reference symbol, a downlink- and an uplink section. The reference symbol is transmitted by the base station (BS) and received by all mobile stations (MS) in the cell, in order to align their carrier frequencies at the commencement of the TDD/TDMA frame[2, 3].

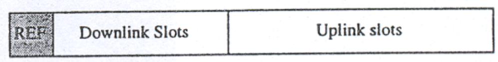

Figure 1: Schematic plot of a time frame of a TDMA/TDD system.

2 Frequency acquisition

The frequency acquisition algorithm has to provide an initial frequency error estimate, which is sufficiently accurate for the subsequent frequency tracking algorithm to support fine tracking, generally to half a subcarrier spacing. Sari [4] proposed the use of a pilot tone embedded into the data symbol. Moose [5] suggested using a shortened repeated OFDM symbol pair, exploiting the phase of the auto-correlation of the received repetitive time-domain signal. Keller [6] advocated the use of a periodic training symbol, in order to increase the frequency capture range of the autocorrelation based algorithms further. Claßen and Meyr [7, 8] proposed to use binary pseudo-noise (PN) or so-called CAZAC training sequences carried by synchronisation subcarriers. Schmidl [9] suggests a blind frequency acquisition algorithm for Phase Shift Keying (PSK) or Star–QAM [10] modulation. Time–domain training sequence based algorithms have been suggested by Lambrette *et al.* [11] and Házy [12].

Our proposed **frequency acquisition algorithm** operates using a reference symbol that is emitted by the base station at the start of each TDMA/TDD frame, as depicted in Figure 1. The reference symbol consists of a set of M pilot tones, spanning the OFDM signal's bandwidth, spaced from each other by ΔN sub-carriers or by a frequency gap of $\Delta F = \Delta N \cdot \Delta f$. Accordingly, the maximum detectable frequency error is $\Delta F/2 =$

*MICROCOLL'99, 22-25 March, 1999, Budapest, Hungary

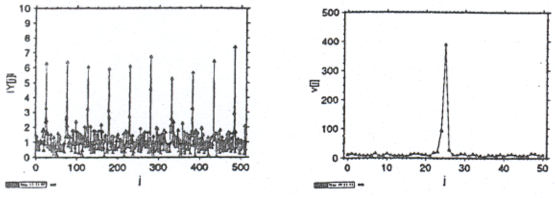

(a) $|Y(j)|$ (b) $V(j)$

Figure 2: Magnitude of $|Y(j)|$ and $V(j)$ for $\gamma = 0$dB and $\delta f = 0.3\Delta f$

$\Delta N/2 \cdot \Delta f$. The total energy of the reference symbol is set equal to the average OFDM symbol energy, and split equally between the M pilot tones.

A frequency mismatch between the transmitter and the receiver results in a shift of the pilot tones in the received spectrum. This frequency shift is estimated at the receiver by searching for the FFT frequency bin having the maximum amplitude, resulting in an estimation accuracy of half a subcarrier spacing. This estimation is improved further by considering the relative amplitudes of the adjacent FFT bins.

The frequency-domain position of the pilot tones is estimated at the receiver after the time–domain signal is demodulated by FFT, as usual. In order to minimise the influence of noise, the sum of the received power spectral amplitudes over all the M frequency ranges is then calculated as follows:

$$V(j) = \sum_{m=0}^{M-1} |Y(j + j_s + m\Delta N)|^2 \quad \text{with} \quad -\frac{\Delta N - 1}{2} \le j \le \frac{\Delta N - 1}{2}, \qquad (1)$$

where $Y(j)$ represents the frequency–domain samples of the received demodulated reference symbol. In Figure 2 simulated values for both $|Y(j)|$ and $V(j)$ are given for a SNR value of 0 dB, given a 10–pilot reference symbol in a 512–subcarrier OFDM system and a frequency error of $\delta f = 0.3\Delta f$. It can be seen that the positions of the pilot tones in the received spectrum are readily determined even for a low SNR of 0 dB, thanks to the high power of the pilot tones relative to the normal data subcarrier power.

The frequency error is determined by estimating the position of the highest peak in $V(j)$ over the range of j given in Equation 1. This provides a rough estimate of the frequency error with a frequency resolution given by the subcarrier spacing Δf. The accuracy of this estimation, however, is insufficient for low–BER modem operation. If a subsequent frequency error tracking algorithm is employed in the system, then the $0.5\Delta f$ estimation accuracy can be an adequate starting point for the tracking algorithm. If a better estimate is needed, however, then the amplitudes in the neighbouring bins around the peak value in $V(j)$ can be exploited as follows.

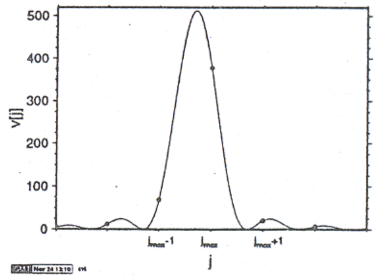

Figure 3: $V(j)$ for $\gamma = 0$dB and $\delta f = 0.3\Delta f$.

The spectral density function of each OFDM subcarrier follows a sinc-shape, centered around the subcarrier frequency [10]. In the presence of a frequency error between the transmitter and receiver, the receiver's sampling raster in the frequency domain is shifted by the frequency error δf. The spectrum of the received reference symbol, containing M pilot tones at the frequencies $(j_s + m\Delta N) \cdot \Delta f$ with $0 \le m \le (M-1)$ will therefore be received with a frequency error δf, but without noise as:

$$Y(j) = \sqrt{\frac{N}{M}} \cdot \sum_{m=0}^{M-1} \operatorname{sinc}\left(j - j_s - m\Delta N + \frac{\delta f}{\Delta f}\right). \qquad (2)$$

The factor $\sqrt{N/M}$ is the amplitude of each pilot tone, ensuring that the overall energy of the reference symbol is equal to the average signal energy. If the frequency distance ΔN between two consecutive pilot tones is sufficiently high, so that the received spectra of the different pilot tones do not overlap significantly, then the vector $V(j)$, as defined by Equation 1, can be approximated as:

$$V(j) \approx M \cdot \operatorname{sinc}^2\left(j + \frac{\delta f}{\Delta f}\right). \qquad (3)$$

Figure 3 shows the simulated values of $V(j)$ for a noiseless case in more detail around the peak, along with the values corresponding to the sinc approximation of Equation 3 represented by the dots, where j_{max} indicates the position of the maximum of $V(j)$. It can be seen that there is a very good correspondence between the simulated and the approximated values for the pilot spacing of $M = 50$ employed in this case.

Using the sinc^2 approximation of Equation 3, the values for $V(j_{max})$, $V(j_{max}+1)$ and $V(j_{max}-1)$ can be expressed in terms of the normalised fine frequency error estimation $\nu = \delta f/\Delta f - j_{max}$:

$$V(j_{max}) \approx N\mathrm{sinc}^2(\nu), \tag{4}$$
$$V(j_{max}+1) \approx N\mathrm{sinc}^2(1+\nu), \quad \text{and} \tag{5}$$
$$V(j_{max}-1) \approx N\mathrm{sinc}^2(-1+\nu). \tag{6}$$

Then the following normalised terms can be defined:

$$\rho_1 = \frac{\sqrt{V(j_{max}+1)}}{\sqrt{V(j_{max})}} \tag{7}$$
$$\approx \frac{\sqrt{N}\,|\sin(\pi(1+\nu))|}{|\pi(1+\nu)|} \cdot \frac{|\pi\nu|}{\sqrt{N}\,|\sin(\pi\nu)|} \tag{8}$$
$$= \frac{|\nu|}{|1+\nu|} \quad \text{and, similarly,} \tag{9}$$
$$\rho_{-1} \approx \frac{|\nu|}{|-1+\nu|}. \tag{10}$$

The value d, defined as half the difference between ρ_1 and ρ_{-1} can be therefore approximated as:

$$d = \frac{\rho_1 - \rho{-1}}{2} \approx \frac{1}{2}\left(\frac{|\nu|}{|1+\nu|} - \frac{|\nu|}{|-1+\nu|}\right). \tag{11}$$

Solving Equation 11 for values of ν smaller than one subcarrier distance yields:

$$\nu = \begin{cases} -\sqrt{\frac{d}{d+1}} & \text{for} \quad -1 < \nu < 0 \quad (\text{or} \quad (d > 0) \\ \sqrt{\frac{d}{d-1}} & \text{for} \quad 0 \leq \nu < 1 \quad (\text{or} \quad d \leq 0) \end{cases} \tag{12}$$

The $V(j)$ peak position estimation can thus be refined, using Equation 12, as follows:

$$\hat{\delta f} = \Delta f \cdot (j_{max} + \nu). \tag{13}$$

A series of simulations was conducted, in order to investigate the performance of this peak position estimation algorithm under noisy conditions for a 512 subcarrier system employing a 10–pilot reference symbol. Histograms of the estimation errors in an AWGN channel for frequency errors of $\delta f = 0$, $\delta f = 0.3\Delta f$ as well as for $\delta f = 0.5\Delta f$ are given in Figure 4. In all cases, the estimation accuracy was better than $0.5\Delta f$, which is sufficiently low for the subsequent fine-tracking algorithm to remove the residual frequency error.

The performance of the algorithm in a Rayleigh fading time dispersive channel is depicted in Figure 4(d). The channel model used is that of an indoors Wireless ATM (WATM) system, operating at 60 GHz with a sample rate of 225 MHz. Figure 5 shows the unfaded impulse response consisting of three paths and the corresponding frequency domain channel transfer function. Each of the paths is multiplied by an independent Rayleigh fading function of a normalised Doppler frequency of $1.235 \cdot 10^{-5}$, which corresponds to a worst-case vehicular velocity of 50 km/h or 13.89 m/s.

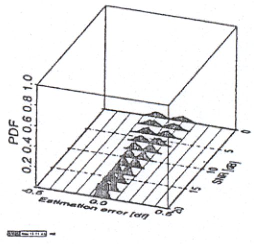

(a) $\delta f = 0$

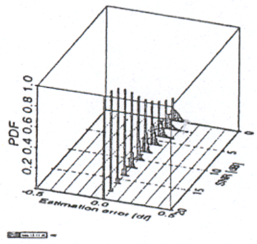

(b) $\delta f = 0.3\Delta f$

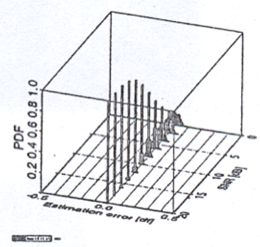

(c) $\delta f = 0.5\Delta f$

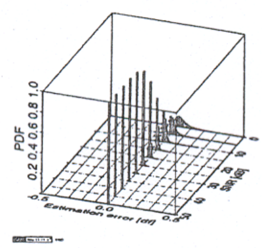

(d) wide-band Rayleigh channel

Figure 4: (a)–(c): Histograms of the estimation error in narrow–band AWGN channel for different frequency errors δf. (d): in the Rayleigh fading time dispersive channel for a frequency error of $\delta f = 0.3\Delta f$

3 System BER performance

In order to investigate the effects of the proposed frequency synchronisation algorithm on an OFDM modem, a series of simulations was conducted over the time dispersive Rayleigh fading channel of Figure 5(a). For each TDD/TDMA frame the frequency acquisition was performed using the proposed reference symbol, and one data symbol was demodulated using the estimated frequency errors. No averaging was performed for the estimated values. The simulated OFDM symbols consisted of a 512 subcarrier data segment, with a cyclic preamble of 64 samples.

Coherently detected Binary Phase Shift Keying (BPSK), Quadrature Phase Shift Keying (QPSK) and 16-Quadrature Amplitude Modulation (16-QAM) were assumed for data transmission over the subcarriers, and the channel transfer function estimation was performed with 64 frequency-domain pilot tones spread across the OFDM bandwidth. A constant frequency error of $\delta f = 0.3\Delta f$ was assumed for the simulations.

The symbols in Figure 6 show the BER performance of the OFDM modem employing the proposed synchronisation algorithm, compared to the ideally synchronised modem with the same pilot based channel

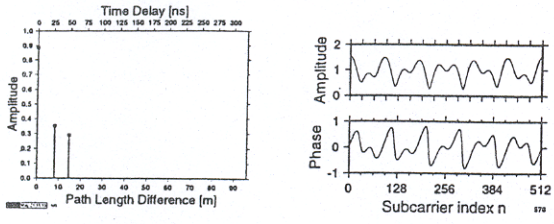

(a) channel impulse response

(b) channel frequency response

Figure 5: Short WATM channel: (a) – impulse response (b) – unfaded frequency domain channel transfer function $H(n)$

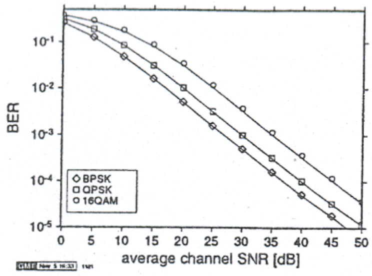

Figure 6: BER versus channel SNR of OFDM modem over the WATM channel of Figure 5(a), both with reference–symbol based and perfect channel estimation

estimation, which is represented by the continuous lines. For all SNR values the perfectly synchronised system performs marginally better than the acquired synchronised one. The difference between the two systems' performance is, however, only marginal for BPSK and QPSK. 16-QAM exhibits a higher sensitivity to synchronisation–errors, and suffers a maximum SNR loss of about 1 dB.

4 Conclusion

In this paper, we have proposed a novel reference symbol assisted frequency acquisition algorithm for TDD/TDMA-based OFDM WATM systems, which operates reliably down to extremely low SNR values, irrespective of the number of bits / symbol transmitted and hence it is applicable to burst-by-burst adaptive OFDM modulation.

5 Acknowledgements

The financial support of Motorola ECID, Swindon, UK and that of the European Commission in the framework of the Median project is gratefully acknowledged.

References

[1] M. v. B. Thierry Pollet and M. Moeneclaey, "BER sensitivity of OFDM systems to carrier frequency offset and Wiener phase noise," *IEEE Trans. on Comm.*, vol. 43, pp. 191–193

[2] W. D. Warner and C. Leung, "OFDM/FM frame synchronization for mobile radio data communication," *IEEE Trans. Veh. Tech.*, vol. 42, August 1993.

[3] K. Brüninghaus and H. Rohling, "Verfahren zur Rahmensynchronisation in einem OFDM-System," in *3. OFDM Fachgespräch in Braunschweig*, 1998.

[4] I. J. Hikmet Sari, Georges Karam, "Transmission techniques for digital terrestrial tv broadcasting," *IEEE Comms. Mag.*, February 1995.

[5] P. H. Moose, "A technique for orthogonal frequency division multiplexing frequency offset correction," *IEEE Trans. on Comm.*, vol. 42, pp. 2908–2914

[6] T. Keller and L. Hanzo, "Orthogonal frequency division multiplex synchronisation techniques for wireless local area networks," in 7^{th} *PIMRC*, (Taipei, ROC), pp. 963–967, IEEE, October 1996.

[7] F. Claßen and H. Meyr, "Synchronisation algorithms for an OFDM system for mobile communications," in *Codierung für Quelle, Kanal und Übertragung*, no. 130 in ITG Fachbericht, (Berlin), pp. 105–113, VDE–Verlag, 1994.

[8] F. Claßen and H. Meyr, "Frequency synchronisation algorithms for OFDM systems suitable for communication over frequency selective fading channels," in *Proc. VTC 1994*, pp. 1655–1659, IEEE.

[9] T. M. Schmidl and D. C. Cox, "Blind synchronisation for OFDM," *Electronics Letters*, vol. 33, pp. 113–114, January 1997.

[10] W. Webb and L. Hanzo, *Modern Quadrature Amplitude Modulation: Principles and Applications for Wireless Communications*. IEEE Press-Pentech Press, 1994.

[11] U. Lambrette, M. Speth, and H. Meyr, "OFDM burst frequency synchronisation by single carrier training data," *Communications Letters*, March 1997.

[12] L. Házy and M. El-Tanany, "Synchronization of OFDM systems over frequency selective fading channels," in *Proc. VTC 1997*, pp. 2094–2098, IEEE.